Multiple jets in the Malvinas Current

Alberto R. Piola,[1,2,3] Bárbara C. Franco,[3,4] Elbio D. Palma,[3,4] and Martín Saraceno[2,3,5]

Received 7 October 2012; revised 18 March 2013; accepted 20 March 2013.

[1] The velocity structure of the Malvinas Current is described based on the analysis of high-resolution hydrographic data and direct current observations. The data show that though the current width exceeds 150 km, the flow is concentrated in two relatively narrow (~10–20 km) jets. Within these cores, the direct observations indicate surface velocities exceeding 0.5 m.s^{-1}. Surface drifter, satellite-derived mean dynamic topography, and sea surface temperature data suggest that the high-velocity jets are also ubiquitous features of the time mean circulation. Both jets appear to be continuous features extending more than 900 km along the western slope of the Argentine Basin. These jets closely follow the 200 and 1400 m isobaths. Additional high-velocity cores are apparent in direct current measurements and hydrographic observations, but these features are weaker and not continuous along the slope. Though the Malvinas Current transport is mostly barotropic, baroclinic jets are also identified in relative geostrophic velocity sections. The baroclinic jets are colocated with the barotropic jets. Our results suggest that the main Malvinas Current core is located over a relatively flat portion of the bottom, referred to as the Perito Moreno terrace. This observation is in agreement with recent seismic and geological evidence suggesting that in geological time scales the Malvinas Current played a key role in the configuration of the bottom sediments over the western slope of the Argentine Basin.

Citation: Piola, A. R., B. C. Franco, E. D. Palma, and M. Saraceno (2013), Multiple jets in the Malvinas Current, *J. Geophys. Res. Oceans*, *118*, doi:10.1002/jgrc.20170.

1. Introduction

[2] Downstream of Drake Passage the northern portions of the Antarctic Circumpolar Current (ACC) make a sharp northward turn and enter the western Argentine Basin to form the Malvinas/Falkland Current (MC). Numerical models suggest that about 50% of the waters within the upper layer limb of the Atlantic Meridional Overturning Circulation are derived from the ACC via the MC [*Friocourt et al*., 2005]. The MC provides the northernmost path of nutrient rich subpolar waters in the southern hemisphere, creating a region of enhanced biological activity [*Longhurst*, 1998] and significant fisheries [*Acha et al*., 2004]. The MC is an intense, equivalent barotropic, and relatively narrow flow that penetrates northward along the western margin of the Argentine Basin to about 38ºS, where it describes a sharp cyclonic loop and returns southward at about 55ºW [*Matano*, 1993; *Peterson and Whitworth*, 1989]. The surface expression of the MC closely follows the path of the Subantarctic Front (SAF) [*Orsi et al*., 1995] (Figure 1) and waters from Polar Front Zone occupy the center of the cyclonic loop [*Piola and Gordon*, 1989]. The southward return flow (hereafter referred to as the Malvinas Return Current – MRC) and the associated SAF merge with the Polar Front north of the Ewing Bank (~ 50ºS–45ºW) and then continue eastward across the South Atlantic. The water masses in the upper and deep layers along the western slope of the Argentine Basin resemble the structure observed in the ACC in the northern Drake Passage [*Peterson and Whitworth*, 1989; *Piola and Gordon*, 1989], but the paths of these waters are strongly controlled by the complex bottom topography of the North Scotia Ridge and the Malvinas/Falkland Plateau. While the upper and intermediate waters flow around Burdwood Bank and along the upper slope of the western Argentine Basin [*Piola and Gordon*, 1989], most of the Upper Circumpolar Deep Water (UCDW) flows through a gap in the North Scotia Ridge located close to 54ºS–54ºW. The denser Circumpolar Deep Water and South Pacific Deep Water make a northward turn passing through the Shag Rocks Passage (Figure 1), and then continue into the Argentine Basin either over or east of the Malvinas/Falkland Plateau [*Arhan et al*., 1999; *Arhan et al*., 2002; *Naveira Garabato et al*., 2002; *Peterson and Whitworth*, 1989; *Smith et al*., 2010]. Still denser waters

Additional supporting information may be found in the online version of this article.

[1]Departamento Oceanografía, Servicio de Hidrografía Naval, Buenos Aires, Argentina.
[2]Departamento Ciencias de la Atmósfera y los Océanos, Facultad de Ciencias Exactas y Naturales, Universidad de Buenos Aires, Argentina and Instituto Franco-Argentino sobre, Estudios de Clima y sus Impactos, CNRS/CONICET, Buenos Aires, Argentina.
[3]Consejo Nacional de Investigaciones Científicas y Técnicas, Buenos Aires, Argentina.
[4]Departamento de Física, Universidad Nacional del Sur, and Instituto Argentino de Oceanografía, Bahía Blanca, Argentina.
[5]Centro de Investigación del Mar y la Atmósfera, UBA/CONICET, Buenos Aires, Argentina.

Corresponding author: A. R. Piola, Departamento Oceanografia, Servicio de Hidrografia Naval, Av. Montes de Oca 2124, C1270ABV, Buenos Aires, Argentina. (apiola@hidro.gov.ar)

2169-9275/13/10.1002/jgrc.20170

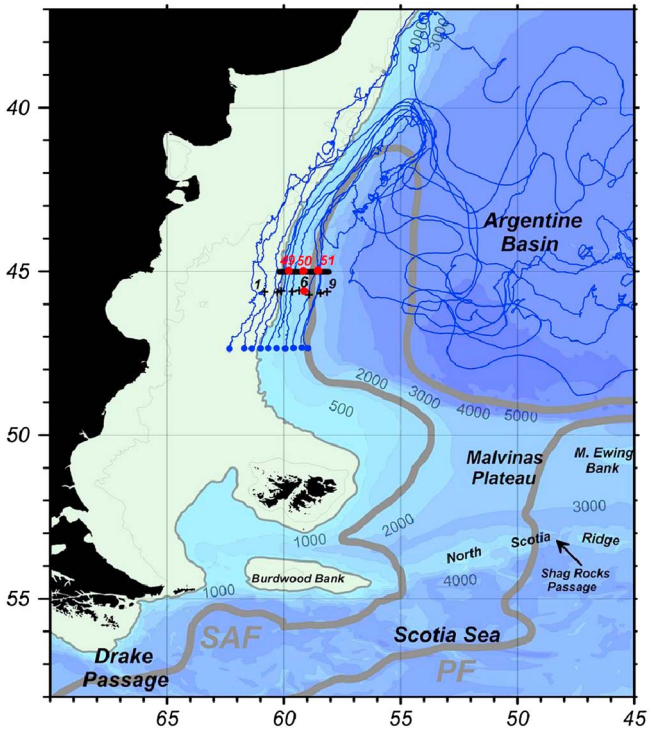

Figure 1. Location of hydrographic stations occupied in September 1997 (+) used to prepare the sections shown in Figure 2. Also shown are the tracks of surface drifters deployed on 16–17 March 2006 (light blue) with deployment positions indicated by filled blue circles. The WOCE A11 ADCP section shown in Figure 3 is indicated by the heavy black line at 45ºS. Red circles indicate the location of hydrographic stations used to prepare Figure 7. The thick gray lines are the Subantarctic Front (SAF) and Antarctic Polar Front (PF), from *Orsi et al*. [1995]. The background shading is the bottom topography, in m.

originated in the Weddell Sea also flow northward along the abyssal portion of the western slope of the Argentine Basin [*Arhan et al*., 1999; *Arhan et al*., 2002; *Georgi*, 1981; *Naveira Garabato et al*., 2002]. South of about 40ºS all water masses flow northward along the western boundary. However, as the deeper flow is constrained by the slope of the seafloor, most of the northward abyssal boundary flow occurs underneath the southward flowing MRC [*Georgi*, 1981; *Peterson and Whitworth*, 1989; *Piola and Gordon*, 1989].

[3] The equivalent barotropic nature of the MC and the steep sloping bottom make it difficult to estimate the associated geostrophic volume transport based on hydrographic observations only. Mass conservation arguments led to a MC volume transport estimate of 70 Sv ($1\,\mathrm{Sv} = 10^6\,\mathrm{m^3.s^{-1}}$) in the upper 2000 m near 46ºS, and somewhat lower figures further north [*Peterson*, 1992]. Though these transports were much larger than previous estimates, *Peterson* [1992] argued that adjusted MC surface velocities were consistent with evidence from satellite tracked drifters. Hydrographic data collected across the MC near 45ºS and adjusted with direct current observations in the upper layer led to a transport estimate of 50 Sv [*Saunders and King*, 1995]. Similarly, direct current measurements combined with satellite altimetry near the northernmost reach of the MC (at 40 – 41ºS) indicate a volume transport of 41.5 ± 12.5 Sv [*Vivier and Provost*, 1999], while a recent analysis of a 14-year altimeter time series, also adjusted by direct current measurements, leads to 35 ± 7.5 Sv [*Spadone and Provost*, 2009]. A moderate-resolution numerical simulation also presents somewhat larger MC mean transports which display a northward decrease from ~ 70 to 54 Sv [*Fetter and Matano*, 2008].

[4] Simplified analytical and numerical models suggest that the MC transport is important in determining the latitude of separation of the Brazil Current from the western boundary [*Agra and Nof*, 1993; *Matano*, 1993]. These models also show that the intense northward flow along the western margin of the Argentine Basin is produced by a bottom trapping effect downstream of Drake Passage, where the flow is strongly constrained to follow lines of constant planetary potential vorticity [*Matano*, 1993]. Such contours provide a direct, though convoluted connection between Drake Passage and the Brazil/Malvinas Confluence. Lagrangian observations suggest that the MC extends vertically at least to 750 m depth on most of its northward extent along the western boundary [*Davis et al*., 1996]. The alignment of surface temperature fronts [*Saraceno et al*., 2004] and of surface drifter trajectories [*Piola et al*., 2010] with lines of constant potential vorticity seems to confirm that the flow approximately conserves potential vorticity. These investigations have considered the MC as a single current; however, a recent study indicates that the surface thermal structure along the western limb of the MC is characterized by multiple fronts [*Franco et al*., 2008]. The analysis of *Franco et al*. [2008] suggests the presence of three branches of cold waters whose edges delineate the above mentioned fronts. In agreement with the results reported by *Saraceno et al*. [2004], the two offshore fronts closely follow lines of constant planetary potential vorticity and appear to be associated with the MC. *Franco et al*. [2008] show that while a shelf break front (SBF) approximately follows the 200 m isobath, from spring to autumn two additional fronts are located ~ 40 km onshore and offshore from the SBF. *Franco et al*. [2008] pointed out that the two offshore fronts follow similar paths of MC branches inferred from quasi-synoptic subsurface density distributions [*Piola and Gordon*, 1989]. The detailed structure of the along-shore velocity is important to better understand the MC dynamics, to quantify its volume transport [*Vivier and Provost*, 1999], and may have significant implications on shelf break upwelling [*Matano and Palma*, 2008] and the redistribution of bottom sediments [*Hernández-Molina et al*., 2009]. The purpose of this article is to analyze the velocity field along the northward path of the Malvinas Current with special attention to the cross-shore structure of the along-shore flow and its possible relationship with the surface fronts and the bottom topography. We also wish to determine whether the surface patterns have a subsurface expression that manifests itself in the velocity structure of the MC. To this end we analyze high-resolution hydrographic sections across the MC together with satellite tracked surface drifters, underway current observations, and satellite altimetry data. Based on the analysis of these data, we will show that the MC is characterized by a set of well-defined high-velocity cores. The paper is organized as follows: the data are described in section 2, in section 3 we present the results, and the discussion and conclusions are presented in sections 4 and 5, respectively.

2. Data and Methods

[5] To display the water mass structure and the baroclinic component of the flow associated with the MC, we use high-resolution quasi continuous conductivity-temperature-depth and water sample data collected on 9–11 September 1997. Upper ocean velocities from a hull mounted acoustic Doppler current profiler (ADCP) and hydrographic data collected in late December 1992 [*Saunders and King*, 1995] are also analyzed. The ADCP data are available through NOAA/NCDDC/University of Hawaii (http://ilikai.soest.hawaii.edu/sadcp/). To illustrate the regional flow patterns in the upper layer, we use satellite tracked surface drifters. The drifters are WOCE-Surface Velocity Program type, drogued at 15 m depth, designed to follow the water to within $\pm$ .013 m.s^{-1} in 10 m.s^{-1} winds [*Niiler et al*., 1995]. The original position data, collected at irregular time intervals, have been quality controlled and optimally interpolated to uniform 6-h interval trajectories [*Hansen and Poulain*, 1996]. The data are available at NOAA's Atlantic Oceanographic and Meteorological Laboratory (AOML, http://www.aoml.noaa.gov/phod/index.php). Only drogued drifters are used in this study. To analyze the regional characteristics of the mean flow, we estimated the surface geostrophic velocity based on satellite altimetry-derived mean dynamic topography (MDT). We use the Danish National Space Center mean dynamic topography model (DNSC08 MDT). DNSC08 MDT is a high-resolution (1 min) global data set constructed from the combination of 12 years (1993–2004) of sea surface height derived from nine satellite missions and a geoid model [*Andersen and Knudsen*, 2009]. The data are available at http://www.space.dtu.dk/. Prior to estimating the mean geostrophic velocity, the MDT data were spatially smoothed with a 20 km low-pass filter. In addition, nighttime MODIS Aqua and Pathfinder version 5 sea surface temperature (SST) data are used to display the cross-slope structure of ocean fronts. These 4 km resolution SST data are available through NASA/Jet Propulsion Laboratory Physical Oceanography Distributed Active Archive Center (http://podaac.jpl.nasa.gov/dataaccess).

3. Results

3.1. Hydrography, Water Masses, and Geostrophic Shear

[6] In this section, the thermohaline structure across the outer continental shelf and slope is illustrated based on a high-resolution hydrographic section occupied at 45.5ºS in September 1997 (Figures 1 and 2), representative of late austral winter conditions. Between stations 4 and 8, the section displays a wedge of relatively cold (potential temperature, $\theta < 5$°C), salty ($S > 34$) waters associated with the MC (Figures 2a and 2b). The outer shelf presents near-surface salinities lower than 33.6 capping a saltier near-bottom layer ($S \sim 33.8$ at station 1, about 50 km inshore from the shelf break). The offshore salinity increase and potential temperature decrease lead to a relatively sharp density increase. It will later be shown that this density front is associated with a geostrophic jet along the upper slope. East of the shelf break, the isotherms and isopycnals rise about 300–500 m in 60–80 km in the offshore direction. The portion of the water column with greatest isopycnal tilt lies underneath the surface temperature minimum ($<$ 5°C, stations 4–7), where the most intense northward flow of the MC is observed (Figure 2d). Surface temperature and salinity increase further offshore and subsurface isotherms and isopycnals flatten out and their tilt reverses in the upper 100 m, as these waters are recirculated southward as part of the MRC. Note that the near-surface waters are warm and saline relative to the MC and shelf waters (Figures 2a and 2b). Temperature and salinity in the upper layer continue increasing eastward, as they present mixtures with subtropical waters from the Brazil/Malvinas Confluence. The above described structure is typical of the late winter situation throughout the shelf break [*Romero et al*., 2006].

[7] We present the structure of the baroclinic velocity field in the slope region based on the geostrophic velocities estimated relative to the deepest common level between adjacent stations for the austral winter section (Figure 2d). No attempt is made here to estimate absolute geostrophic velocities. The baroclinic velocity displays a well-defined jet (B in Figure 2d) with surface velocities exceeding 0.35 m.s^{-1}, centered about 80 km east of the shelf break, close to station 6. This high-speed core extends vertically to about 900 m and is associated with the region of maximum isotherm and isopycnal tilt observed west of station 8. In addition, two distinct high-velocity cores are apparent in Figure 2d. First, a near-surface core (A) with a surface velocity of 0.2 m.s^{-1} is located 20 km east of the shelf break. This core is limited to the upper 100 m and is associated with the density front observed at the shelf break between stations 3 and 4. The relatively steep bottom slope between stations 3 and 4 prevents calculating the geostrophic shear below 205 m without substantial vertical extrapolations at station 3. Thus, it is likely that the estimated baroclinic shear and the vertical extent of this high-velocity core are underestimated. A third high-velocity core (C) is located 140 km east of the shelf break (station pair 8-9, Figure 2d). This core occupies the 300 to 1000 m depth range, with velocities exceeding 0.1 m.s^{-1}. The high-velocity core C appears to be associated with the differential isopycnal tilt between the upper 150 m and the layers underneath (Figure 2c). Given that the baroclinic shear is much weaker than in cores A and B, no definitive conclusion on the existence of core C can be drawn from the hydrographic section. Summer hydrographic data from a section collected at 43°S also present a main MC core and a secondary onshore core, both being displaced ~50 km onshore from the winter location (not shown).

[8] There are various shortcomings associated with the geostrophic velocity estimates in the MC. First, based on the analysis of hydrographic data combined with mass conservation arguments and direct current measurements, studies suggest that the barotropic transport of the MC is three to four times larger than its baroclinic counterpart [*Peterson*, 1992; *Saunders and King*, 1995; *Spadone and Provost*, 2009]. Second, the steep bottom slope creates large "bottom triangles" within which we lack information on the density structure and therefore also velocity estimates. The later problem is somewhat circumvented by reducing the station separation, but for instance, in the upper slope, where the bottom drops from 230 to 785 m in less than 14 km, resolving this steep slope would require station separations of only a few km. Therefore, any attempt to better determine the geostrophic velocity based on hydrographic data requires

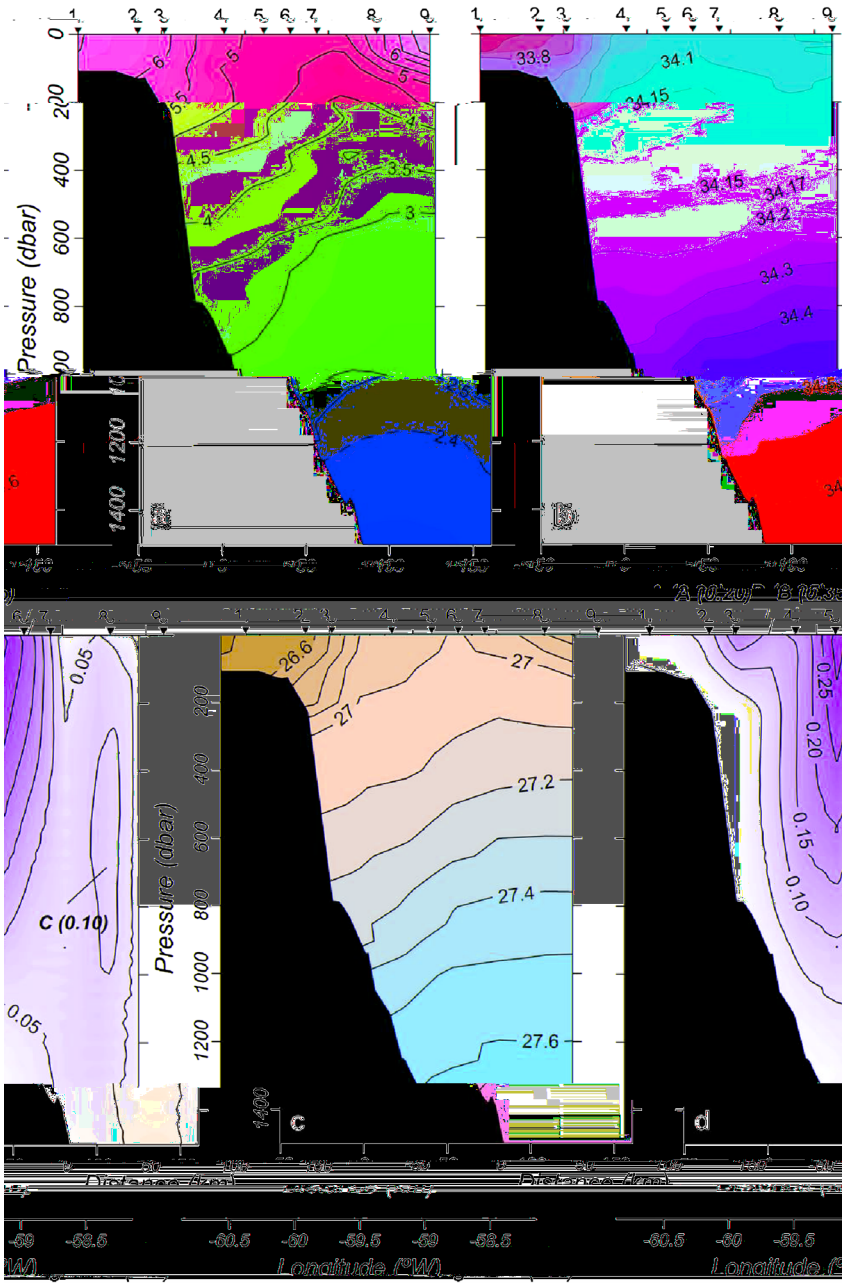

Figure 2. (a, °C) Potential temperature, (b) salinity, (c, kg.m^{-3}) potential density anomaly, and (d, m.s^{-1}) relative geostrophic velocity near 45.5ºS. High-velocity jets A-C are indicated (see text). The stations were occupied on 9–11 September 1997. Cross-shore distances (km) are relative to the shelf break. Station locations are indicated in Figure 1.

substantial vertical extrapolations of the shallow station density structure, or adjusting the velocity field based on direct observations.

3.2. Upper Layer Current Measurements

[9] The first direct current observations of the Malvinas Current in the upper layer were obtained from RSS Discovery in late December 1992 during WOCE cruise A11 [*Saunders and King*, 1995]. Fitted with a hull mounted 150 KHz ADCP the vessel crossed the current at 45ºS in a westward course and returned eastward occupying hydrographic stations. The observed current patterns on these two crossings were remarkably similar, with small (~ 0.05 m.s^{-1}) fluctuating differences mostly attributable to semi-diurnal tides [*Saunders and King*, 1995]. The ADCP meridional velocity component in the 30– 390 m depth interval presents an energetic northward flow spanning nearly 150 km between 58ºW and the shelf break (~60ºW), with peak near-surface velocities of ~0.8 m.s^{-1} (Figure 3b). The ADCP data reveal that the northward flow is concentrated in two jets within which velocities are > 0.5 m.s^{-1}. The main jet is centered at 59.12ºW; about 70 km east of the shelf break, where the bottom depth is ~1400 m, while a secondary jet is observed ~10 km offshore from the shelf break. The main MC jet is

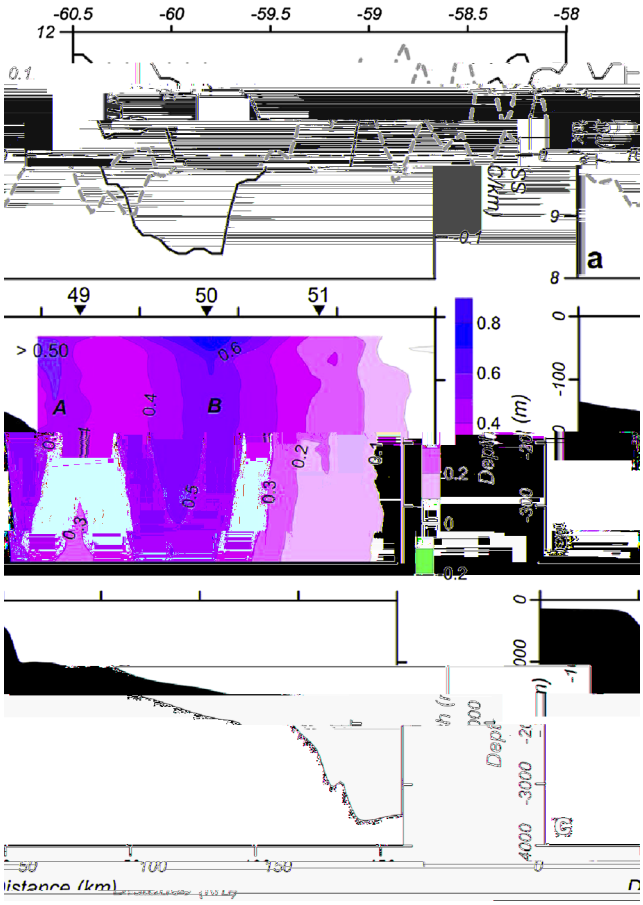

Figure 3. (a) Satellite-derived sea surface temperature (solid line, left axis, °C) and zonal temperature gradient (dashed line, right axis, °C.km^{-1}) from Pathfinder v. 5 along 45ºS on 24 December 1992. (b) Meridional velocity (m.s^{-1}) section along 45ºS from a hull mounted acoustic Doppler current profiler collected on 28 December 1992 from RSS Discovery during WOCE A11. (c) Bottom topography (m).

surface intensified with velocity decreasing from 0.83 m.s^{-1} at 30 m to 0.58 m.s^{-1} at 100 m, though at 390 m, the velocity is still quite high (0.49 m.s^{-1}). The ADCP velocity shear in the 100 – 390 m depth interval is virtually identical to the hydrography-derived geostrophic shear depicted in Figure 2d (see Figure S1, supporting information). The secondary jet (A) located close to the continental shelf break presents lower velocities than its offshore counterpart (B), but appears to similarly extend downward beyond the ADCP range, which displays velocities exceeding 0.40 m.s^{-1} at the deepest bin centered at 390 m. Figure 3 also suggests that the inshore jet may not have been fully sampled during the A11 cruise; particularly, the highest surface velocities may be located further inshore.

[10] A recent survey conducted on R/V Roger Revelle in late 2008 and early 2009 in the outer shelf and slope regions collected several additional MC velocity sections across the slope also employing a 150 KHz hull mounted ADCP [*Painter et al*., 2010]. These data show a broad along isobath flow closely following the western slope of the Argentine Basin. In agreement with the early ADCP observations of *Saunders and King* [1995], the recent observations also display multiple, vertically coherent, high-velocity cores at various sections occupied between 42.5 and 52ºS [*Painter et al*., 2010]. At 45ºS, a narrow (~ 15 km) high-velocity (> 0.5 m.s^{-1}) core is observed against the slope, while a wider (35 km) and less intense (0.35 m.s^{-1}) core is centered at 59.2ºW. The two jets in the late 2008 survey are observed virtually at the same locations as in 1993, though the offshore jet appears to be significantly weaker in the most recent survey. Two additional high-velocity cores at 45ºS (~ 0.2 m.s^{-1}) are apparent in the 2008 ADCP survey: one is located over the outer shelf (at 60.5ºW) and the other close to 58.1ºW [*Painter et al*., 2010 their Figure 6]. These cores are much weaker and somewhat narrower than jets A and B and do not seem to be continuous in the along-shore direction. Further upstream, near 47.5ºS, the ADCP data display two high-velocity jets [*Painter et al*., 2010 their Figure 6]; a narrow (~ 20 km) onshore core (> 0.3 m.s^{-1}) is located at the upper slope (60.8ºW) and a substantially wider offshore core (> 0.5 m.s^{-1}) about 120 km further east of the shelf break (near 59.3ºW). In this case, the jets are separated by a 45 km band of very low (< 0.1 m.s^{-1}) northward velocities and narrow regions of southward flow. Thus, the ADCP data collected in 2008 suggest that the high-velocity cores observed in the upper slope may be continuous features of the circulation extending from about 52ºS (their leg P-Q) to at least 42ºS (their leg C-B).

3.3. Surface Drifters

[11] Further evidence of the existence of multiple high-velocity cores in the MC comes from the analysis of near-surface velocities from WOCE surface velocity program drifters. Figure 4 depicts the meridional velocity from all observations available across the continental slope at various latitude ranges. As the isobaths converge northward, near 43.5ºS, it is difficult to distinguish the dual jet structure of the MC based on the surface drifters (Figure 4a). Further south, however, the drifter data clearly display a double jet structure in the surface layer (Figures 4b, 4c, and 4d). At ~ 45.8ºS between the outer shelf and 57ºW and within this latitude range, there are 888 6-hourly velocity estimates derived from the location of 80 surface drifters, which have been collected between April 1994 and July 2011. Although the velocity estimates at any given longitude present substantial variations, the overall structure of the MC is apparent, with the flow extending about 160 km east of the shelf break (Figure 4b). This current width agrees well with the above described ADCP surveys. Mean meridional velocities estimated over 0.2º longitude bins (~ 14–16.2 km each) and standard deviations are also shown in Figure 4. West of the onshore edge of the MC at 45.8ºS, the meridional velocity increases sharply from about 0.05–0.15 m.s^{-1} in the outer shelf to > 0.6 m.s^{-1} close to the shelf break. This onshore peak is narrow (< 50 km) and centered at 60.1ºW. A broader velocity maximum (~ 0.5 m.s^{-1}) is centered at 59.3ºW. A narrow strip of lower meridional velocity (~ 0.3 m.s^{-1}) separates the above mentioned maxima. Further east, the meridional velocity decreases sharply, and east of 58.2ºW, it is highly variable with the mean reversing to southward, indicative of the MRC. This location of the MRC is about 270 km west of the climatological location of the SAF determined by *Orsi et al*. [1995] and 190 km west of its location derived from satellite altimetry [*Sokolov and Rintoul*, 2009].

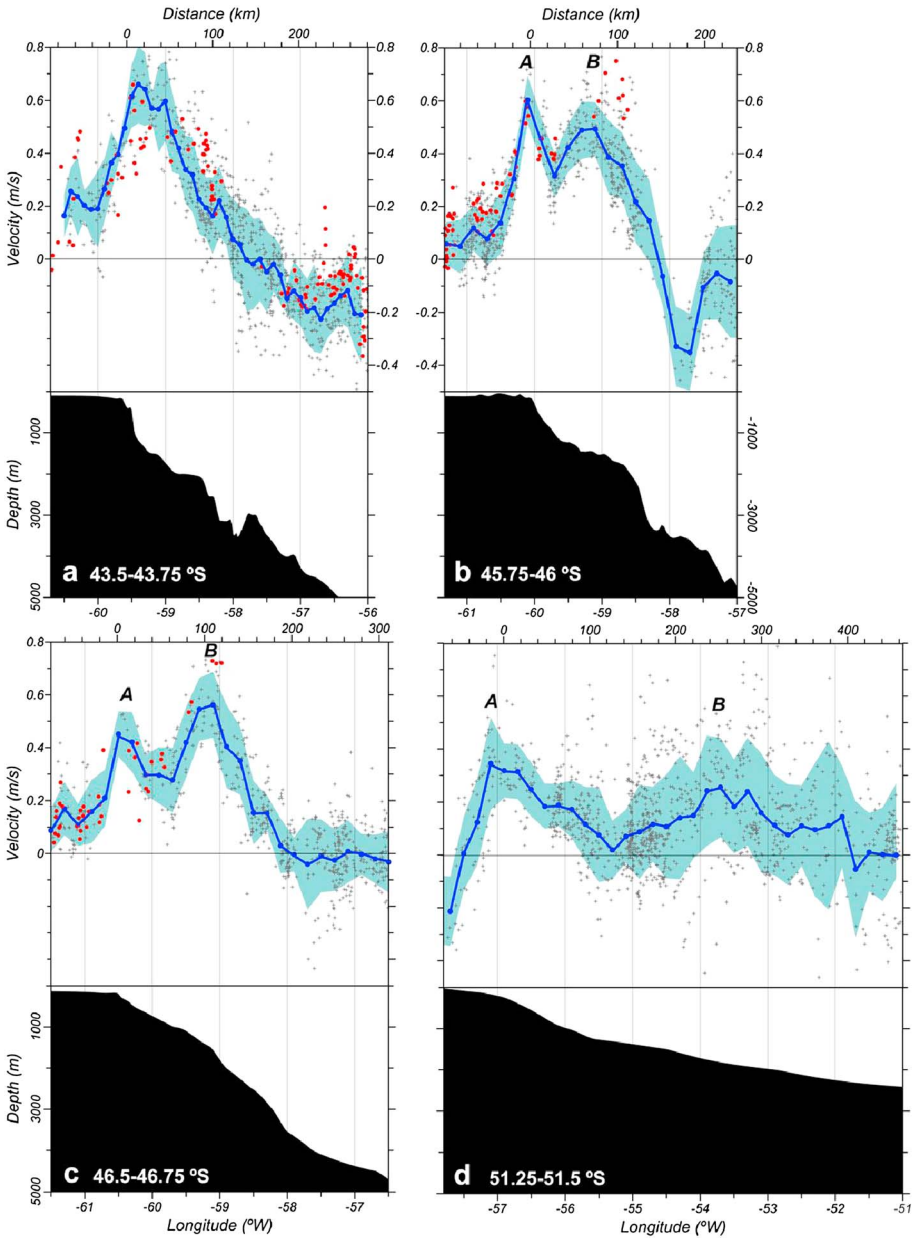

Figure 4. Meridional surface velocity (+, $m.s^{-1}$) estimated from all available satellite tracked drifter trajectories collected between (a) 43.5–43.75ºS, (b) 45.75–46ºS, (c) 46.5–46.75ºS, and (d) 51.25–51.5ºS. The blue dots and line indicate the mean velocities binned in 0.2º longitude intervals. Standard deviations around each mean are indicated by the background shading. Meridional surface velocities from drifters deployed on 16–17 March 2006 as they crossed each latitude band (●) are also shown in Figures 4a–4c. Jets A and B are indicated in Figures 4b–4d.

Interestingly, however, near 45ºS the transition from northward to southward flow derived from both ADCP surveys, and the surface drifters (Figure 4) is located near 58ºW. This implies that the surface cyclonic loop is significantly narrower than suggested by the climatological frontal locations. Our conclusion is in agreement with the observation near 58ºW of an intense surface SST transition between the cold MC and the warmer return flow [*Saraceno et al.*, 2004]. The double jet structure is also evident at 46.7ºS (Figure 4c). Though at the southernmost section, near 51.3ºS, the MC flow is much wider (~ 400 km), and presents lower and more variable surface velocities, two regions of relatively high velocity are still apparent (Figure 4d). One is centered close to the shelf break (0.35 $m.s^{-1}$ at 57ºW) and another about 270 km offshore (0.25 $m.s^{-1}$ at 53.5ºW). The width of the MC and the high-velocity cores may be linked to the much lower bottom slope at this location. Though the variability in the offshore region is also significantly larger than observed further north (Figures 4b and 4c), the observed pattern is similar to the ADCP line occupied in that region in 2008 [*Painter et al.*, 2010, their leg P-Q].

[12] Because the drifter sampling is very inhomogeneous in space and time, it is useful to further inspect the drifter data to determine the robustness of the two-jet structure.

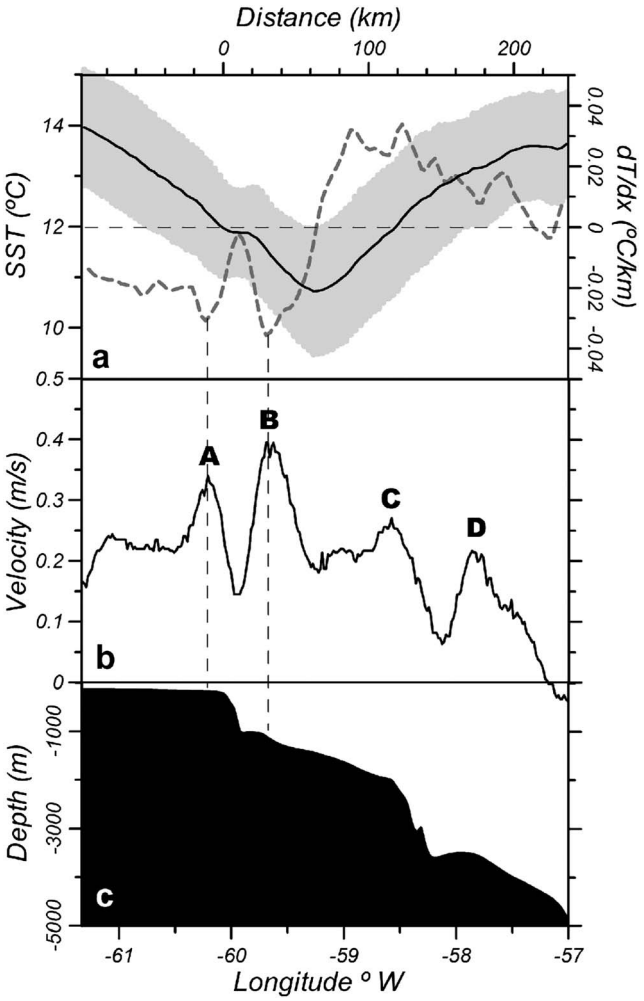

Figure 5. (a) January climatological sea surface temperature (SST) (solid line, left axis, °C) and zonal SST gradient (dashed line, °C.km^{-1}, right axis) at 45ºS from MODIS 4 km nighttime data. The gradient data have been smoothed with a 5 point running mean. The shading represents the standard deviation of the mean SST. (b) Meridional geostrophic velocity component at 45ºS as determined from the DNSC08 high-resolution mean dynamic topography [*Andersen and Knudsen*, 2009]. High-velocity cores are indicated as A-D. (c) Bottom topography (m).

On 16 and 17 March 2006, we deployed ten WOCE SVP surface drifters spanning the outer shelf and slope along 47ºS. The deployment sites and drifter tracks are shown in Figure 1. These data provide a quasi-instantaneous Lagrangian view of the near-surface velocity field across the MC between 47ºS and the separation from the slope near 40ºS. After deployment, all instruments drifted closely following the shelf break orientation and describing relatively smooth trajectories. Similarly smooth trajectories are typical of the southwestern edge of the Argentine Basin [*Piola et al*., 2010]. The stability of the MC flow is clearly depicted by a wedge of high mean kinetic energy per unit mass (~ 1000 cm^2.s^{-2}) and low eddy kinetic energy (< 15 cm^2.s^{-2}) derived from the analysis of surface drifters [*Oliveira et al*., 2009], as well as by low rms sea surface height and eddy kinetic energy from satellite altimetry [*Goni et al*., 2011; *Saraceno and Provost*, 2012]. Similarly low eddy kinetic energy is indicated by high-resolution numerical simulations [*Palma et al*., 2008, their Figure 3b]. The meridional velocities of the set of drifters deployed in March 2006 as they crossed various latitude bands are plotted in Figure 4. Though during this particular period, the velocities throughout the slope are quite variable, they are in overall agreement with the velocities from historical drifter observations. For instance, near 46ºS (Figure 4b), there is a clear increase from velocity values lower than 0.3 m.s^{-1} west of 60.5ºW to higher than 0.6 m.s^{-1} at 60.1ºW. The velocity presents a similarly sharp eastward decrease to < 0.4 m.s^{-1} at 59.7ºW. There is a data gap from the later minimum to an offshore maximum (~ 0.6 m.s^{-1}) centered around 100 km east of the shelf break. This later velocity maximum is somewhat more intense and located further offshore than the long-term mean. Nevertheless, the drifter velocity estimates from March 2006 are in close agreement with the velocity structure displayed in the long-term mean, further suggesting the stability of the cross-shore structure of surface along-shore velocity.

3.4. MDT

[13] To further explore the cross-shore velocity structure of the MC, we analyzed the geostrophic velocity derived from a high-resolution (1 min) gridded MDT field. The MDT was constructed by combining satellite altimeter data collected by various platforms from 1993 to 2004, and a global geoid model [*Andersen and Knudsen*, 2009]. The DNSC08 MDT provides the high spatial resolution required to resolve the rather thin high-velocity cores (~10–20 km) apparent in the hydrographic, ADCP, and drifter data. Figure 5b displays the zonal distribution of the meridional velocity component at 45ºS. The mean meridional velocity increases from ~ 0.1 m.s^{-1} in the mid shelf (west of 62ºW, not shown in Figure 5) to 0.22 m.s^{-1} in the outer shelf (61ºW) and presents two sharp peaks that exceed 0.3 m.s^{-1}, one located at 60.2ºW, just onshore from the shelf break, and one at 59.6ºW, where the bottom depth is 1180 m (A and B in Figure 5b). The velocity decreases further offshore, presenting two additional peaks (> 0.2 m.s^{-1}) located at 58.6 and 57.85ºW (C and D, Figure 5b). In contrast with the surface drifter velocities (Figure 4b), the MDT-derived velocities depict the MRC centered on 55ºW, thus, the southward flow is not fully apparent in Figure 5. The discrepancy between different velocity estimates east of the MC might be expected as in this region there is a sharp increase in eddy energy and sea surface height variability [*Goni et al*., 2011; *Saraceno and Provost*, 2012], which also leads to more variable drifter velocities east of 57.5ºW (Figure 4b).

[14] The 1 min gridded DNSC08 MDT data have been smoothed using a correlation length of 75 km [*Andersen and Knudsen*, 2009]. Consequently, the amplitude of the associated geostrophic velocities, which are a function of the spatial derivative of MDT, is reduced. Moreover, the global estimated error of the MDT is about 9–12 cm [*Andersen and Knudsen*, 2009]. A 10 cm uncertainty across a zonal span of 30 km, the cross-slope scale of the velocity peaks estimated at 45ºS, leads to a geostrophic velocity uncertainty of about 0.33 m.s^{-1}, which is close to the amplitude of the velocity peaks themselves (~ 0.35–0.40 m.s^{-1}, Figure 5). Thus, the evidence derived from the MDT analysis on the velocity structure of

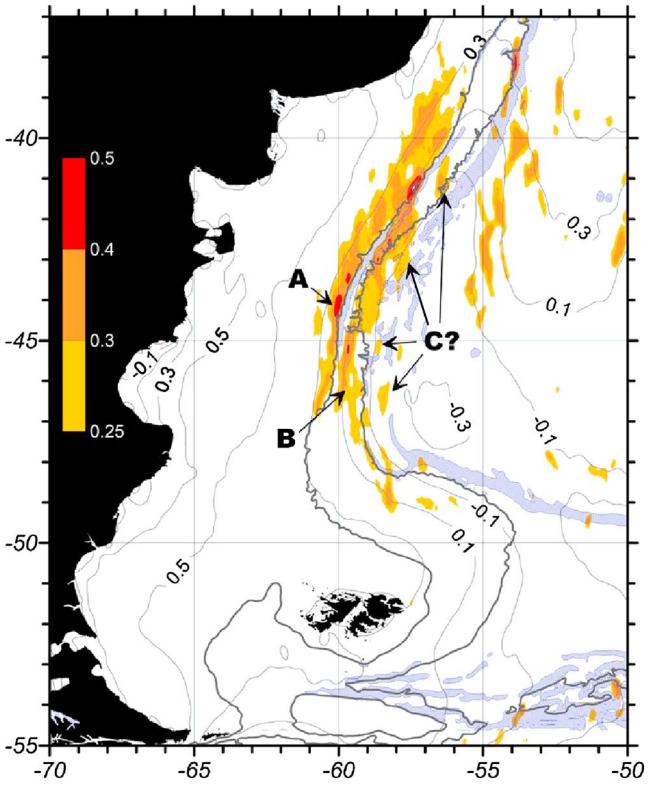

Figure 6. Magnitude of the surface geostrophic velocity ($m.s^{-1}$) as determined from the DNSC08 high-resolution mean dynamic topography [*Andersen and Knudsen*, 2009]. The mean dynamic topography is shown by the thin contours. High-velocity cores are indicated as A-C. The blue hatching indicates region where the bottom slope is $> 35\ m.km^{-1}$ and the heavy gray lines are the 200 and 1500 m isobaths.

the MC is far from conclusive. However, we argue that the qualitative agreement with the upper layer velocity structure indicated by other data suggests that the MDT-derived velocity peaks are a real feature of the ocean circulation at this location. In addition, the MDT dual jet configuration extends along-slope more than 900 km, between 47 and 39.5ºS (Figure 6). The southern portion of this latitude band lies within the multiple jet structure that emerges from the late 2008 ADCP survey across the MC [*Painter et al*., 2010].

3.5. MC Jets and SST Fronts

[15] Given the previous observation of SST fronts associated with the MC [*Franco et al*., 2008] in this section, we explore the possible association between the surface fronts and jets. For this purpose, the January climatological SST distribution at 45ºS is shown in Figure 5a. The mean is calculated from 8-day, 4 km resolution MODIS Aqua far IR nighttime images during the 7-year period 2003–2009. At 45ºS, the SST minimum characteristic of the MC is centered at 59.25ºW, where the bottom is ~1425 m deep, and about 65 km offshore from the shelf break. The zonal SST gradient (T_x), estimated using a centered difference of the 4 km data and smoothed with a 5 point (~ 20 km) running mean, is also shown in Figure 5a. T_x presents two well-defined minima ($< -0.03°C.km^{-1}$), indicative of relatively sharp SST drops in the offshore direction, observed at 60.25 and 59.7ºW. The location of these high-gradient bands is in agreement with the analysis of *Franco et al*. [2008]. These gradient minima are colocated with the maximum MDT-derived meridional velocities, suggesting that the time-averaged SST fronts are associated with high-velocity cores of the MC as depicted by the MDT (Figure 5a and b).

[16] Further insight on the association between MC fronts and jets is gained from the combined analysis of the A11 ADCP section and the concurrent satellite-derived SST. The cross-shore SST pattern based on data collected along the A11 track on 24 December 1992 (Figure 3a) is in good qualitative agreement with the January climatological distribution (Figure 5a): a temperature minimum centered at 59.25ºW, a westward increase, and a relatively narrow isothermal band at the shelf break (~ 60ºW). West of 59ºW, two SST gradient minima are apparent, which correspond to the multiple frontal structures of *Franco et al*. [2008]. In contrast with the MDT-derived velocities, the high-velocity cores as observed during the late 1992 survey are aligned with the two isothermal regions, not the SST minima (Figure 3).

4. Discussion

[17] The analyses of surface drifters and the MDT data, and the agreement between ADCP surveys in the slope area suggest that the MC is characterized by a relatively stable multiple jet structure. To display the regional distribution of the MC jets, we present the horizontal distribution of the magnitude of the surface velocity (V) derived from the DNSC08 MDT (Figure 6). This distribution reveals two distinct high-velocity cores (~ $0.4\ m.s^{-1}$) each extending more than 900 km from 47.5ºS to about 39ºS along the western boundary (Figure 6). Moreover, Figure 6 shows that the two most intense jets observed at 45ºS (A and B, Figure 5b) are quasi-continuous features observed along the slope. The onshore jet (A) is located just onshore of the 200 m isobath, while the offshore jet (B) follows the 1000 m isobath south of 45ºS and the 1500 m isobath further north. Further offshore the V distribution also displays other high-velocity regions, but these cores are discontinuous based on the MDT (Figure 6).

[18] Because of the equivalent barotropic nature of the MC, volume transport estimates based on integral observations, such as those provided by "density" moorings and geostrophic calculations, lead to a small (baroclinic) fraction of the actual transport [e.g., *Peterson*, 1992]. Therefore, estimates of the total transport require direct current observations [*Saunders and King*, 1995; *Vivier and Provost*, 1999]. The multiple jet structure of the MC may have a substantial impact on transport estimates based on direct current measurements. For example, the total northward transport estimated west of 58ºW over the 30–400 m depth range covered by the ADCP data from A11 is 20.8 Sv, with 7.2 Sv, or 34% being contributed by two 20 km bands associated with jets A (3.2 Sv) and B (4.0 Sv, Figure 3). Thus, failure to properly resolve the MC velocity structure would lead to gross errors in total MC transport estimates.

4.1. MC Jets and ACC Fronts

[19] The MC and its southward return are closely associated with the SAF [*Peterson and Whitworth*, 1989]. Thus, it is useful to determine if the MC jets and correlated fronts are associated with the SAF. The location of the SAF can be

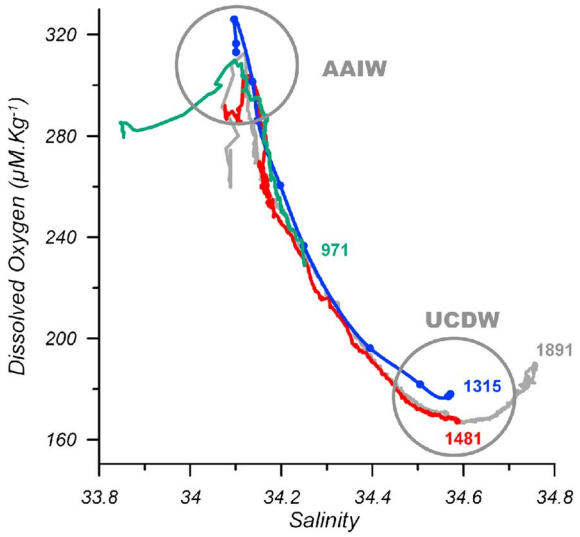

Figure 7. Salinity versus dissolved oxygen distribution of stations 49 (green), 50 (red), and 51 (gray) occupied during WOCE A11 section, and station 6 occupied in September 1997 (blue dots). The depth of the deepest sample (m) is shown for each station. The core characteristics of Antarctic Intermediate Water (AAIW) and Upper Circumpolar Deep Water (UCDW) are indicated. Station locations are shown in Figure 1.

determined based on the following indicators: $S < 34.20$ at depth < 300 m and dissolved oxygen > 7.1 ml.l^{-1} at depth 200 m south of the SAF; and $\theta > 4$–5°C at 400 m, north of the SAF [*Orsi et al*., 1995]. Figure 2a indicates that in September 1997 the $\theta = 4$°C surface is at 400 m depth between stations 5 and 6, very close to the high-velocity core B and over the 1400 m isobath. The salinity distribution (Figure 2b) shows that all waters shallower than 500 m are fresher than 34.2; thus, the salinity criterion is not useful to determine the location of the SAF across the MC. As *Orsi et al*. [1995] pointed out, due to the regional variability around the ACC, not all the frontal indicators may apply at some particular location. This thermal SAF identification criterion differs slightly from the one proposed by *Peterson and Whitworth* [1989], who traced the frontal location in the western Argentine Basin where the 4°C isotherm is located at 200 m depth, which lies close to station 7 during the September 1997 survey.

[20] A recent analysis of Southern Ocean fronts based on satellite altimetry data has shown that the ACC can be characterized by nine frontal regions, each associated with high sea surface height gradients, high-velocity cores, and specific ACC streamlines [*Sokolov and Rintoul*, 2009]. The study indicates that the SAF is characterized by three distinct fronts and that the main SAF intrudes northward into the western Argentine Basin similarly to the SAF pattern described by *Orsi et al*. [1995]. The analysis of *Sokolov and Rintoul* [2009] indicates that the SAF-north, which is characterized by $\theta \sim 6.1 - 6.3$°C at 400 dbar, diverges from the main path of the ACC turning northward along the west coast of South America. Indeed, these waters are too warm to be observed at 400 dbar in the northern Drake Passage or along the MC, where such temperatures can only be attained after mixing with warm-salty subtropical waters within the MRC (e.g., downstream of the Brazil/Malvinas Confluence). Similarly, the SAF-south, associated with $\theta \sim 2.65 - 2.78$°C at 400 dbar, is too cold to intrude along the cyclonic MC loop [*Orsi and Whitworth*, 2005; *Peterson and Whitworth*, 1989], its mean northernmost position downstream of Drake Passage lies over the Malvinas/Falkland Plateau [*Sokolov and Rintoul*, 2009]. Thus, it appears that only the main SAF, which is presumably associated with jet B, diverts northward along the western boundary of the Argentine Basin. This suggests that the multiple thermal fronts observed along the northward path of the MC are not associated with the secondary frontal structures that characterize the SAF at circumpolar scale.

4.2. Interaction Between MC Jets and the Seafloor

[21] The bottom topography appears to effectively control the path of the MC along the continental margin of the western Argentine Basin. At 45ºS, the position of the main MC jet (B) derived from hydrography (Figure 2), ADCP surveys (Figure 3), and surface drifters (Figure 4) lies about 60–70 km east of the continental shelf break, close to the 1400 m isobath. The bottom at this location is relatively flat compared to the steep slopes found at either side (Figure 3c). Adjusting the relative geostrophic shear derived from a hydrographic section with the cross-shore structure of the along-shore velocity determined from the observed displacements of seven drifters drogued at 100 m depth, *Peterson et al*. [1996] estimated the velocity structure across the MC at 42ºS. In agreement with our findings, their study indicates that the MC core is located over a relatively flat portion of the slope where the bottom depth is 1400 m. This relatively flat portion of the slope is found at a depth similar to the Perito Moreno terrace, which extends from 50 to 45ºS [*Hernández-Molina et al*., 2009]. In contrast with the above observations, the MDT-derived jet (B) lies about 35 km further onshore, at around 59.6ºW (e.g., at the western edge of the above described terrace, Figures 5 and 6). The cause of this discrepancy in the jet location is unclear, it is possible that the long-term mean is well represented by the MDT (1993–2004), but it may also arise from the interpolation and smoothing of the altimeter data required to produce the DNSC08 MDT over a regular grid, or from geoid uncertainties. In any case, all the data sets we analyzed locate jet B on the Perito Moreno terrace, or at about 1400 m further north.

[22] To determine the extent of the relationship between the location of the MC jets and the bottom topography, the slope of the bottom topography as determined from the GEBCO Digital Atlas 0.5 min resolution data [*IOC et al*., 2003] is superimposed to the altimeter-derived velocities in Figure 6. This comparison indicates that the transitions between jets approximately follow the high-gradient regions, therefore suggesting that the high-velocity cores, even considering the jet location uncertainties indicated above, tend to be located over the less steep portions of the slope (i.e., terraces).

[23] Recent studies have suggested that over geological time scales the intense boundary currents of the western Argentine Basin have effectively reworked and redistributed the bottom sediments leading to the formation of a large contourite depositional system [*Hernández-Molina et al*., 2009]. These studies argue that the evolution and present

morphology of the margin results from the action of near-bottom currents flowing along the slope. *Hernández-Molina et al*. [2009] identified four such terraces and suggested these features are formed by erosive processes associated with water mass interfaces. The Perito Moreno terrace is presumably associated with the Antarctic Intermediate Water-UCDW interface at a depth of ~1 km [*Hernández-Molina et al*., 2009; *Preu et al*., 2013].

[24] *Peterson* [1992] estimated the bottom velocities along the slope required to compensate the large offshore geostrophic flow inferred from quasi-synoptic observations between 38 and 42ºS. In the upper slope, at 42 and 46ºS and between 1000 and 2000 m depth, his estimates indicate bottom speeds of 0.18- 0.23 $m.s^{-1}$. These velocity estimates are somewhat lower than the 0.35 $m.s^{-1}$ inferred between 1500 and 2000 m in a high-resolution numerical simulation [*Palma et al*., 2008]. Though our velocity estimates do not extend to the near-bottom layer, in agreement with previous observations [*Saunders and King*, 1995; *Spadone and Provost*, 2009; *Vivier and Provost*, 1999], our results indicate that the velocity structure along the MC axis is coherent in the upper 1000 m (Figure 2d). Thus, our data suggest that the Perito Moreno terrace is associated with the main MC jet (B). To evaluate the hypothesized relationship between the near-bottom flow and the near-bottom water characteristics, Figure 7 presents a salinity-dissolved oxygen ($S-O_2$) scatter diagram for stations occupied close to jet B as determined from direct ADCP observations collected during WOCE A11 (December 1992, station 50), and from the September 1997 hydrographic survey (station 6). The station locations are shown in Figure 1. These stations reached within 16 and 41 m from the seafloor, respectively. The $S-O_2$ space allows for a clear identification of the cores of the fresh, oxygen-rich Antarctic Intermediate Water and the low-oxygen UCDW. For reference, stations immediately onshore and offshore of jet B are also shown in Figure 7. The $S-O_2$ diagram shows that in both occupations, the near-bottom waters close to jet B correspond to the oxygen minimum that characterizes the core of UCDW (Figure 7). However, it is important to note that the station occupied in December 1992 lies 10 km east of the high-velocity core, where the bottom is about 40 m deeper. Interestingly, though at 45ºS, the Perito Moreno terrace appears to match the core of UCDW within jet B, the onshore end of the terrace, where the bottom depth is about 1000 m, shows near-bottom characteristics associated with the AAIW-UCDW interface (station 49 in Figure 7), as postulated by *Hernández-Molina et al*. [2009]. Finally, it is important to note that the terraces in the western Argentine Basin present depth discontinuities associated with complex cross-slope and along-slope canyons. Across these discontinuities the depth of the terraces change along the margin [e.g., *Hernández-Molina et al*., 2009; *Preu et al*., 2013] and as the Perito Moreno terrace rises it is likely it becomes in contact with the AAIW-UCDW interface. These small-scale topographic features are likely to locally alter the near-bottom flow patterns.

5. Conclusions

[25] In this article, we have combined a variety of in situ and satellite data to describe the cross-shore velocity structure of the Malvinas Current along the western margin of the Argentine Basin. These data indicate that the flow is characterized by two distinct and continuous jets closely associated with the bottom topography. In addition, the data also suggests the existence of a series of secondary and discontinuous high-velocity cores.

[26] Surface drifters display an inshore jet with surface velocities $> 0.5–0.6\ m.s^{-1}$ located close to the continental shelf break. Another surface jet presenting similarly high velocities approximately follows the 1400 isobath. These two surface jets appear to converge downstream (~ 40ºS), in agreement with the convergence of isobaths in the upper continental slope. Geostrophic velocities derived from hydrographic data suggest that the high-velocity cores have a weak but discernable baroclinic component matching the location of the surface jets. The vertical shear, extent, and location of the jets are also confirmed by direct shipboard velocity measurements. Based on recent underway velocity observations, the multiple jets in the upper layer have a meridional extent of about 900 km, between 42.5 and 52°S. In accordance with the ADCP survey and surface drifters, the analysis of a high-resolution MDT derived from satellite altimetry reveals that two distinct and continuous high-velocity cores extend from about 47ºS to 42ºS. The jets are separated by a region of relatively steep bottom slope, which suggests a close relationship with the bottom topography. The altimetric expression of the onshore core is observed onshore of the 200 m isobath while the offshore core is located close to the 1500 m isobath. The location of the offshore core, which we refer to as the main Malvinas Current jet, lies on top of the Perito Moreno terrace, a significant feature of a large contourite depositional system of the western Argentine Basin [*Hernández-Molina et al*., 2009]. These results highlight the importance of high quality underway current observations to better understand the details of the velocity field in energetic currents. Attempts to determine the MC transport from direct current measurements must be carefully designed to properly resolve its jet-like structure. In addition, the agreement between direct current observations (derived from drifters and ADCP) and those derived from sea surface height observations suggests a remarkable improvement of satellite altimeter products in recent years.

[27] **Acknowledgments.** This research was funded by grant CRN2076 from the Inter-American Institute for Global Change Research, which is supported by the US National Science Foundation (Grant GEO-0452325), MINCYT/CONAE grant 001 and ANPCyT grant PICT08-1874. B.C.F. was supported by a fellowship from Consejo Nacional de Investigaciones Científicas y Técnicas, Argentina. Comments from three anonymous referees are gratefully acknowledged.

References

Acha, E. M., H. W. Mianzan, R. A. Guerrero, M. Favero, and J. Bava (2004), Marine fronts at the continental shelves of austral South America: Physical and ecological processes, *J. Mar. Syst.*, *44*(1-2), 83–105.

Agra, C., and D. Nof (1993), Collision and separation of boundary currents, *Deep Sea Res. Part I*, *40*(11-12), 2259–2282.

Andersen, O. B., and P. Knudsen (2009), DNSC08 mean sea surface and mean dynamic topography models, *J. Geophys. Res.*, *114*, C11001, doi:10.1029/2008JC005179.

Arhan, M., K. J. Heywood, and B. A. King (1999), The deep waters from the Southern Ocean at the entry to the Argentine Basin, *Deep Sea Res. Part II*, *46*(1-2), 475–499.

Arhan, M., A. C. Naveira Garabato, K. J. Heywood, and D. P. Stevens (2002), The Antarctic Circumpolar Current between the Falkland Island and South Georgia, *J. Phys. Oceanogr.*, *32*(6), 1914–1931.

Davis, R. E., P. D. Killworth, and J. R. Blundell (1996), Comparison of Autonomous Lagrangian Circulation Explorer and fine resolution Antarctic model results in the South Atlantic, *J. Geophys. Res.*, *101*(C1), 855–884.

Fetter, A. F. H., and R. P. Matano (2008), On the origins of the variability of the Malvinas Current in a global, eddy-permitting numerical simulation, *J. Geophys. Res.*, *113*, C11018, doi:10.1029/2008JC004875.

Franco, B. C., A. R. Piola, A. L. Rivas, A. Baldoni, and J. P. Pisoni (2008), Multiple thermal fronts near the Patagonian shelf break, *Geophys. Res. Lett.*, *35*, L02607, doi:10.1029/2007GL032066.

Friocourt, Y., S. Drijfhout, B. Blanke, and S. Speich (2005), Water Mass Export from Drake Passage to the Atlantic, Indian, and Pacific Oceans: A Lagrangian Model Analysis, *J. Phys. Oceanogr.*, *35*(7), 1206–1222.

Georgi, D. T. (1981), Circulation of bottom waters in the southwestern South Atlantic, *Deep Sea Res. Part A*, *28*(9), 959–979.

Goni, G. J., F. Bringas, and P. N. DiNezio (2011), Observed low frequency variability of the Brazil Current front, *J. Geophys. Res.*, *116*, C10037, doi:10.1029/2011JC007198.

Hansen, D. V., and P.-M. Poulain (1996), Quality Control and Interpolations of WOCE-TOGA Drifter Data, *J. Atmos. Oceanic Technol.*, *13*(4), 900–909.

Hernández-Molina, F. J., M. Paterlini, R. Violante, P. Marshall, M. de Isasi, L. Somoza, and M. Rebesco (2009), Contourite depositional system on the Argentine Slope: An exceptional record of the influence of Antarctic water masses, *Geology*, *37*(6), 507–510.

IOC, IHO, and BODC (2003), Centenary Edition of the GEBCO Digital Atlas, edited, Intergovernmental Oceanographic Commission and the International Hydrographic Organization as part of the General Bathymetric Chart of the Oceans, British Oceanographic Data Centre.

Longhurst, A. (1998), *Ecological Geography of the Sea*, 560 pp., Academic Press, San Diego.

Matano, R. P. (1993), On the separation of the Brazil Current from the coast, *J. Phys. Oceanogr.*, *23*(1), 79–90.

Matano, R. P., and E. D. Palma (2008), On the upwelling of downwelling currents, *J. Phys. Oceanogr.*, *38*(11), 2482–2500.

Naveira Garabato, A. C., K. J. Heywood, and D. P. Stevens (2002), Modification and pathways of Southern Ocean Deep Waters in the Scotia Sea, *Deep Sea Res. Part I*, *49*(4), 681–705.

Niiler, P. P., A. S. Sybrandy, K. Bi, P. M. Poulain, and D. Bitterman (1995), Measurements of the water-following capability of holey-sock and TRISTAR drifters, *Deep Sea Res. Part I*, *42*(11-12), 1951–1955, 1957–1964.

Oliveira, L. R., A. R. Piola, M. M. Mata, and I. D. Soares (2009), Brazil Current surface circulation and energetics observed from drifting buoys, *J. Geophys. Res.*, *114*, C10006, doi:10.1029/2008JC004900.

Orsi, A. H., and T. Whitworth III (2005), Hydrographic Atlas of the World Ocean Circulation Experiment (WOCE), vol. 1, *Southern Ocean*, edited by M. Sparrow, P. Chapman, and J. Gould, 23 pp., International WOCE Project Office, Southampton, U.K.

Orsi, A. H., T. Whitworth III, and W. D. Nowlin Jr. (1995), On the meridional extent and fronts of the Antarctic Circumpolar Current, *Deep Sea Res. Part I*, *42*(5), 641–673.

Painter, S. C., A. J. Poulton, J. T. Allen, R. Pidcock, and W. M. Balch (2010), The COPAS-08 expedition to the Patagonian Shelf: Physical and environmental conditions during the 2008 coccolithophore bloom, *Cont. Shelf Res.*, *30*(18), 1907–1923.

Palma, E. D., R. P. Matano, and A. R. Piola (2008), A numerical study of the Southwestern Atlantic Shelf circulation: Stratified ocean response to local and offshore forcing, *J. Geophys. Res.*, *113*, C11010, doi:10.1029/2007JC004720.

Peterson, R. G. (1992), The boundary currents in the western Argentine Basin, *Deep Sea Res. Part A*, *39*(3-4), 623–644.

Peterson, R. G., and T. Whitworth (1989), The Subantarctic and Polar Fronts in relation to deep water masses through the southwestern Atlantic, *J. Geophys. Res.*, *94*(C8), 10,817–10,838.

Peterson, R. G., C. S. Johnson, W. Krauss, and R. E. Davis (1996), Lagrangian measurements in the Malvinas Current, in *The South Atlantic Present and Past Circulation*, edited by G. Weffer, W. H. Berger, G. Siedler and D. J. Webb, pp. 239–247, Springer Verlag, Berlin, Heidelberg.

Piola, A. R., and A. L. Gordon (1989), Intermediate waters in the southwest South Atlantic, *Deep Sea Res. Part A*, *36*(1), 1–16.

Piola, A. R., N. Martínez Avellaneda, R. A. Guerrero, F. P. Jardón, E. D. Palma, and S. I. Romero (2010), Malvinas-slope water intrusions on the northern Patagonia continental shelf, *Ocean Sci.*, *6*(1), 345–359.

Preu, B. F., J. Hernández-Molina, R. Violante, A. R. Piola, C. M. Paterlini, T. Schwenk, I. Voigt, S. Krastel, and V. Spiess (2013), Morphosedimentary and hydrographic features of the northern Argentine margin: the interplay between erosive, depositional and gravitational processes and its conceptual implications, *Deep Sea Res. Part I*, *75*, 157–174.

Romero, S. I., A. R. Piola, M. Charo, and C. A. E. Garcia (2006), Chlorophyll-a variability off Patagonia based on SeaWiFS data, *J. Geophys. Res.*, *111*, C05021, doi:10.1029/2005JC003244.

Saraceno, M., and C. Provost (2012), On eddy polarity distribution in the Southwestern Atlantic, *Deep Sea Res. Part I*, *69*(11), 62–69.

Saraceno, M., C. Provost, A. R. Piola, J. Bava, and A. Gagliardini (2004), Brazil Malvinas Frontal System as seen from 9 years of advanced very high resolution radiometer data, *J. Geophys. Res.*, *109*, C05027, doi:10.1029/2003JC002127.

Saunders, P. M., and B. A. King (1995), Bottom currents derived from a shipborne ADCP on WOCE cruise A11 in the South Atlantic, *J. Phys. Oceanogr.*, *25*(3), 329–347.

Smith, I. J., D. P. Stevens, K. J. Heywood, and M. P. Meredith (2010), The flow of the Antarctic Circumpolar Current over the North Scotia Ridge, *Deep Sea Res. Part I*, *57*(1), 14–28.

Sokolov, S., and S. R. Rintoul (2009), Circumpolar structure and distribution of the Antarctic Circumpolar Current fronts: 2. Variability and relationship to sea surface height, *J. Geophys. Res.*, *114*, C11019, doi:10.1029/2008JC005248.

Spadone, A., and C. Provost (2009), Variations in the Malvinas Current volume transport since October 1992, *J. Geophys. Res.*, *114*, C02002, doi:10.1029/2008JC004882.

Vivier, F., and C. Provost (1999), Volume transport of the Malvinas Current: Can the flow be monitored by TOPEX/POSEIDON?, *J. Geophys. Res.*, *104*(C9), 21105–21122.